to detect for certain such a small anisotropy as this. We conclude, therefore, that there is no conclusive evidence in favour of either a single- or two-position model and that with the large thermal vibrations any such distinction becomes rather meaningless. It would be of the greatest interest to re-examine this substance at a low temperature in order to determine whether the apparent isotropy of the central hydrogen atom is maintained.

We thank Mr R. F. Dyer for his help with the neutron intensity measurements and Mr S. A. Wilson for growing the single crystals. We are grateful to Dr J. C. Speakman, who first aroused our interest in this compound.

References

BACON, G. E. & CURRY, N. A. (1956a). Acta Cryst. 9, 82.

BACON, G. E. & CURRY, N. A. (1956b). Proc. Roy. Soc. A, 235, 552.

BACON, G. E. & DYER, R. F. (1955). J. Sci. Instrum. 32, 256.

BACON, G. E. & PEASE, R. S. (1953). Proc. Roy. Soc. A, 220, 397.

CRUICKSHANK, D. W. J. (1949). Acta Cryst. 2, 65.

HADZI, D. & NOVAK, A. (1955). Nuovo Cim. No. 3 of Supplement to vol. 2, p. 715.

PETERSON, S. W. & LEVY, H. A. (1952). J. Chem. Phys. 20, 704.

SPEAKMAN, J. C. (1949). J. Chem. Soc. p. 3357.

The Crystal Structure of N,N'-Hexamethylenebispropionamide

BY L. H. JENSEN

Department of Anatomy, University of Washington, Seattle, Washington, U.S.A.

SAMUEL KRIMM, ROBERT G. PARRISH* AND DARWIN L. WOOD†

Harrison M. Randall Laboratory of Physics, University of Michigan, Ann Arbor, Michigan, U.S.A.

The crystal structure of N,N'-hexamethylenebispropionamide has been determined by two-dimensional projections. The structure consists of molecules bound together by N–H · · · O bonds to form molecular ribbons. Relatively weak lateral forces operate to bind each molecular ribbon to its neighbors. Cutting properties of the crystals vary markedly with direction and correspond to the anisotropy of intermolecular forces.

Bond lengths and angles have been determined and are close to expected values, except for the appreciably short C–C bonds within the chain. A possible explanation for the apparent shortening is advanced.

Introduction

The molecular structure of simple compounds containing the peptide (–NHCO–) group is of considerable interest in connection with the structure of proteins. It is also important to know the structure of the peptide group for purposes of infra-red spectroscopic studies from which the location of transition moment directions with respect to the bond directions within the group may be determined. In this connection a study of the crystal structure of N,N'-hexamethylenebispropionamide (hereafter referred to as HMBPA) was undertaken.

* Now at the Textile Fibers Department, The E. I. DuPont DeNemours Company, Wilmington, Delaware, U.S.A.

† Now at Bell Telephone Laboratories, Inc., Murray Hill, New Jersey, U.S.A.

Experimental

Unit-cell parameters were determined from rotating-crystal and precession photographs using Cu $K\alpha$ radiation:

$$a_0 = 18.60, b_0 = 4.96, c_0 = 7.49 \text{ Å}, \beta = 97° 15'.$$

The $h0l$ and $0k0$ reflections were extinguished for h odd and k odd respectively. Hence the space group was assumed to be $P2_1/a$. With two molecules per unit cell, $d_{calc.} = 1.11$ g.cm.$^{-3}$.

Crystals of HMBPA in the form of needles or plates can be grown from chloroform solutions. From solutions using a mixed solvent of carbon tetrachloride and chloroform, well formed equilateral parallelopipeds are obtained.

The intermediate axis of the refractive index ellipsoid is coincident with the needle axis, the direction of

most rapid crystal growth. Cleavage at 38° to the surface of the plates is prominent. The cleavage section contains both the axis of intermediate refractive index and the obtuse bisectrix and is, therefore, a principal optical section. The refractive indices are:

$$\alpha = 1\cdot574\pm0\cdot005, \quad \beta = 1\cdot592\pm0\cdot005, \quad \gamma = 1\cdot80\pm0\cdot05 .$$

Cylindrical single crystals having the cylinder axis coincident with the needle axis [010] are readily cut without distortion, using an ordinary histological microtome. This method was not, however, satisfactory for cutting cylinders with axis coincident with [001]. The reason (see below) stems from the relatively great force binding the molecules together in molecular ribbons along b compared to the weak lateral forces between adjacent ribbons. Thus the force to move the microtome blade through the crystal, even for cuts of 1μ depth, was sufficient to cause the crystal to pull apart in the region next to its adhesive mounting. It was found that excellent cylinders along [001] could be cut using a string moistened with chloroform (McGuire, 1949; Maddin & Asher, 1950). The device could also be used for dressing the crystal to size and removing irregularities.

Photographic intensity data were collected using an integrating Weissenberg camera (Wiebenga & Smits, 1950). Data for the $h0l$ reflections were collected from three essentially cylindrical crystals of diameter 0·3, 0·15 and 0·01 mm. Data for the $hk0$ reflections were collected from a single cylindrical crystal 0·2 mm. in diameter. Integrated intensities were determined as described previously (Jensen, 1956) except that in this case the output from the densitometer was recorded by a potentiometric recorder having a logarithmic response so that areas could be determined directly on the chart. In this way 135 of the 179 accessible $h0l$ reflections and 94 of the 118 accessible $hk0$ reflections were observed.

Determination of the structure

The frequency and dichroism of the NH and CO stretching bands in the infra-red spectrum indicate that all the peptide groups are hydrogen bonded with the bond directions within 10° of [010]. Polarized spectra recorded from sections cut parallel and perpendicular to the cleavage planes indicate that the molecules are planar and parallel to the cleavage. Since there are two molecules in the unit cell while $P2_1/a$ has four general positions, it follows that the molecules must lie in special positions. From the very intense 401 reflection, it is clear that the molecules must lie near this plane. This is supported by the fact that the cleavage direction as well as the principal directions coincide with the 401 plane. A trial structure was therefore proposed with the plane of the molecule in this plane. Inclination of the axis of the molecule to the ac plane was estimated from the polarized infra-red data on the hydrogen bonds. Structure factors were calculated and an F_o synthesis on (010) was evaluated, using precession data only. The resulting low-resolution synthesis indicated the essential correctness of the trial structure. Recalculation of the complete set of F_{h0l} for the Weissenberg data resulted

Table 1. Reliability indices

	R_{h0l} (%)	R_{hk0} (%)
Final	7·6	9·0
H atoms omitted	12·9	12·7
Isotropic temperature factor, exp $[-4\cdot0 \sin^2 \theta/\lambda^2]$	15·9	17·7
H atoms omitted, isotropic temperature factor, exp $[-4\cdot0 \sin^2 \theta/\lambda^2]$	20·8	20·7

Table 2. Temperature-factor parameters*

$$\exp -[(B+C\cos^2\varphi)\sin^2\theta/\lambda^2]$$

	B_{h0l} (Å²)	C_{h0l} (Å²)	B_{hk0} (Å²)	C_{hk0} (Å²)
C_1	3·2	3·0	2·9	2·5
C_2	3·2	3·0	2·9	2·5
C_3	3·2	3·0	2·9	2·5
C_4	2·6	3·0	2·7	2·1
C_5	3·5	3·5	4·0	2·1
C_6	4·5	3·5	5·0	2·1
N	3·2	3·0	2·8	2·6
O	4·6	3·2	2·6	4·4

* Direction of maximum vibration for projection on (010) assumed to be +37·5° from a; for projection along [001] assumed to be parallel to a^*.
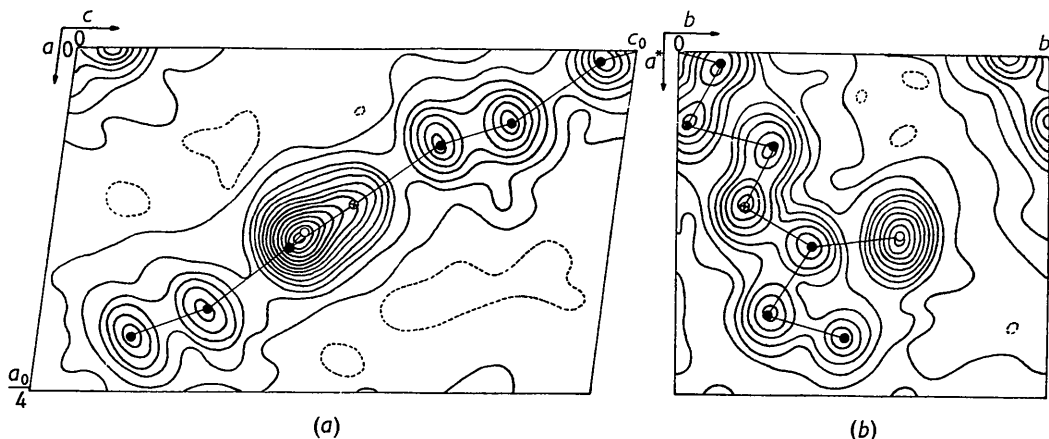

Fig. 1. F_o syntheses: (a) projected on (010); (b) projected along [001]. Contours at integral values of electron density, zero contour broken.
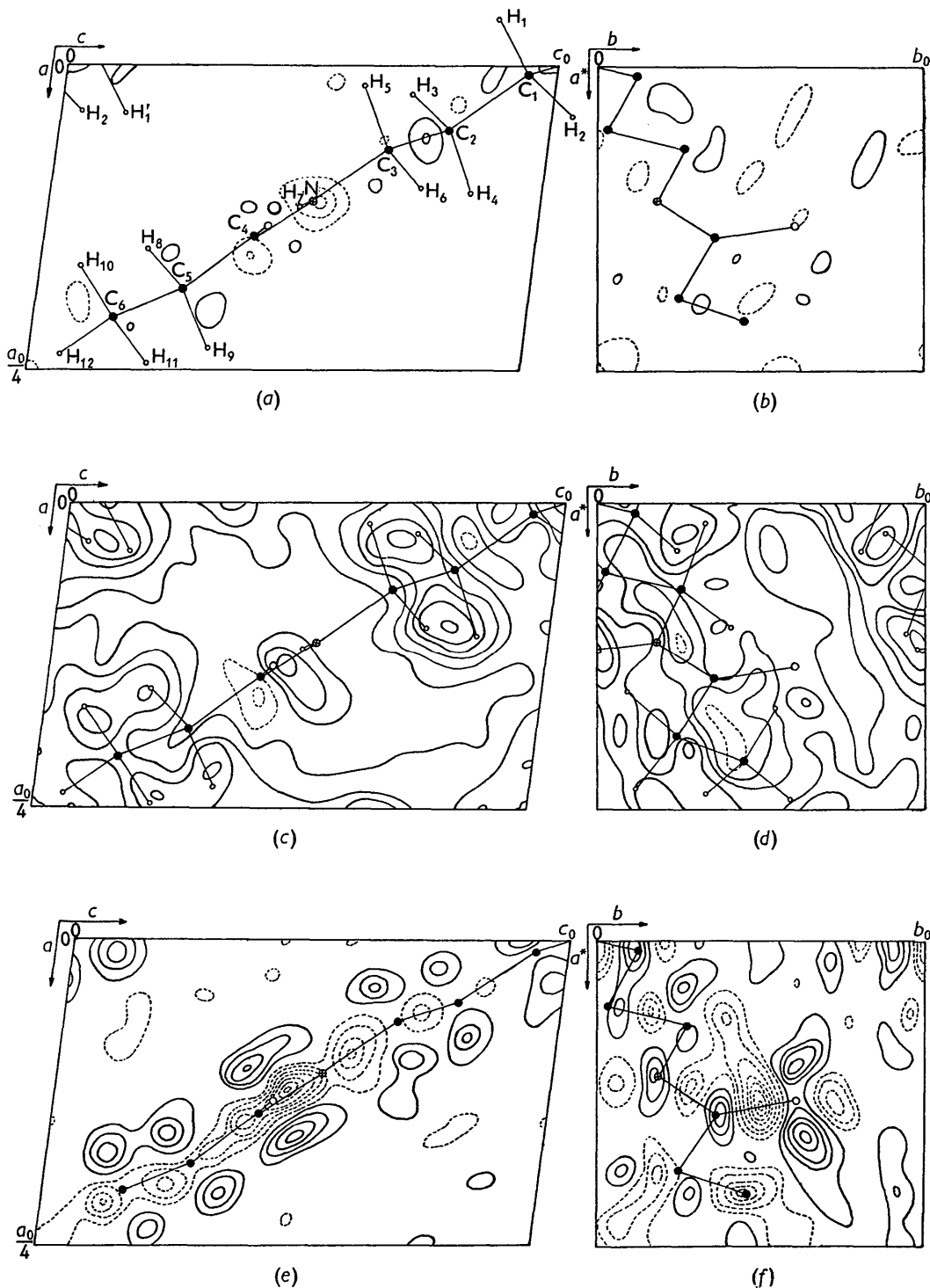
Table 3. *Comparison of observed and calculated structure factors*

Index	Fo	Fc	ΔF
200	17.9	16.9	1.0
400	31.2	-31.7	0.5
600	9.8	7.7	2.1
800	13.0	14.2	-1.1
1000	<1.5	0.5	—
1200	12.6	-12.2	-0.4
1400	8.2	8.1	0.1
1600	9.0	8.8	0.2
1800	<1.7	0.7	—
2000	2.3	1.4	0.9
2200	<1.2	0.0	—
001	44.8	-46.1	1.3
201	9.8	6.7	3.1
401	136.0	149.2	13.2
601	12.8	10.3	2.5
801	16.1	-18.6	0.5
1001	2.5	0.2	2.3
1201	5.9	5.8	0.1
1401	<1.6	0.7	—
1601	5.1	-5.1	0.0
1801	4.4	4.3	0.1
2001	3.8	4.0	-0.2
2201	<1.1	0.6	—
002	13.8	14.7	-0.9
202	21.7	20.3	1.4
402	38.2	-40.6	2.4
602	<1.1	-1.9	0.8
802	50.6	53.4	-2.8
1002	7.4	6.9	0.5
1202	4.8	-4.3	-0.5
1402	<1.7	-0.5	—
1602	2.0	1.2	0.8
1802	<1.6	0.6	—
2002+	1.6	-1.8	0.2
2202	2.2	1.7	0.5
003	22.1	-22.3	0.2
203	9.3	-10.1	0.8
403	16.4	17.5	-1.1
603	12.2	11.1	1.1
803	17.7	-18.3	0.6
1003	<1.5	-1.0	—
1203	18.4	20.1	-1.7
1403	4.2	3.5	0.7
1603	<1.7	-0.3	—
1803	<1.5	-0.3	—
2003	<1.1	0.4	—
004	10.5	10.4	0.1
204	13.2	12.7	0.5
404	11.5	-11.1	-0.4
604	6.5	-6.7	0.2
804	7.4	7.4	0.0
1004	5.3	5.2	0.1
1204	6.3	-6.9	0.6
1404	<1.7	-0.4	—
1604	6.5	6.4	0.1
1804	1.5	1.3	0.2
2004	<0.8	0.0	—
005	4.3	4.4	0.1
205	5.5	-5.5	0.0
405	2.0	2.0	0.0
605	5.0	5.2	-0.2
805	4.9	-4.1	-0.8
1005	3.6	-3.1	-0.5
1205	2.8	3.0	-0.2
1405	2.1	2.1	0.0
1605	2.0	-2.3	0.3
1805	<0.9	-0.2	—
006	1.7	1.0	0.7
206	3.9	4.0	-0.1
406	<1.7	-1.9	0.2
606	2.6	-2.2	-0.4
806	1.7	-1.0	—
1006	1.8	1.3	0.5
1206	2.3	-1.7	-0.6
1406	1.8	-1.4	-0.4
1606	<0.9	1.2	-0.3

Index	Fo	Fc	ΔF
007	<1.7	1.8	-0.1
207	4.1	-4.5	0.4
407	<1.7	1.0	—
607	1.7	1.8	-0.1
807	<1.5	-0.3	—
1007	<1.4	-0.9	—
1207	<1.1	-1.0	—
1407	<0.7	0.4	—
008	7.9	-8.8	0.9
208	6.4	-6.3	-0.1
408	<1.4	0.1	—
608	1.6	-2.4	0.8
808	1.1	0.5	—
1008	<0.8	0.7	—
009	1.6	1.4	0.2
209	1.8	2.1	-0.3
409	3.2	-4.3	1.1
$\bar{3}$01	22.5	20.8	1.7
$\bar{1}$01	5.0	6.3	-1.3
$\bar{5}$01	4.9	4.5	0.4
$\bar{8}$01	24.6	-25.5	0.9
$\bar{10}$01	19.1	17.3	1.8
$\bar{12}$01	17.4	16.0	1.4
$\bar{14}$01	1.5	-1.2	-0.3
$\bar{16}$01	<1.7	0.3	—
$\bar{18}$01	1.8	0.7	1.1
$\bar{20}$01	2.8	-2.5	-0.3
$\bar{22}$01	<1.3	-0.4	—
$\bar{3}$02	<0.8	-0.3	—
$\bar{4}$02	28.2	-28.3	0.1
$\bar{6}$02	36.5	36.7	-0.2
$\bar{8}$02	35.2	32.9	2.3
$\bar{10}$02	3.6	-3.6	0.0
$\bar{12}$02	2.2	-2.0	-0.2
$\bar{14}$02	4.3	3.4	0.9
$\bar{16}$02	3.4	-3.2	-0.2
$\bar{18}$02	2.3	-1.3	-1.0
$\bar{20}$02	2.9	3.2	-0.3
$\bar{22}$02	2.3	-2.2	-0.1
$\bar{2}$03	30.1	29.4	0.7
$\bar{4}$03	32.0	31.5	0.5
$\bar{6}$03	5.7	-5.0	-0.7
$\bar{8}$03	6.6	-5.6	-1.0
$\bar{10}$03	7.2	6.7	0.5
$\bar{12}$03	3.1	-3.1	0.0
$\bar{14}$03	5.8	-4.0	-1.8
$\bar{16}$03	6.2	5.6	0.6
$\bar{18}$03	5.3	-6.0	0.7
$\bar{20}$03	5.3	-5.3	0.3
$\bar{22}$03	<1.2	-0.2	—
$\bar{2}$04	8.0	-7.7	-0.3
$\bar{4}$04	9.3	-8.4	-0.9
$\bar{6}$04	6.7	9.2	-0.5
$\bar{8}$04	<1.4	-1.8	0.4
$\bar{10}$04	10.2	-8.7	-1.5
$\bar{12}$04	9.9	9.5	0.4
$\bar{14}$04	11.0	-11.0	1.6
$\bar{16}$04	10.3	-10.2	0.1
$\bar{18}$04	<1.6	0.0	—
$\bar{20}$04	<1.4	0.7	—
$\bar{22}$04	1.7	0.9	0.8
$\bar{2}$05	7.5	7.9	-0.4
$\bar{4}$05	2.2	0.8	1.4
$\bar{6}$05	12.7	-10.8	-1.9
$\bar{8}$05	9.4	10.0	-0.6
$\bar{10}$05	14.0	-15.5	1.5
$\bar{12}$05	16.5	-15.9	0.6
$\bar{14}$05	2.2	1.7	0.5
$\bar{16}$05	<1.6	0.9	—
$\bar{18}$05	3.0	2.0	1.0
$\bar{20}$05	3.8	-2.8	-1.0
$\bar{22}$05	<0.5	0.9	-0.4

Index	Fo	Fc	ΔF
$\bar{2}$06	7.8	-7.6	-0.2
$\bar{4}$06	4.8	5.3	-0.5
$\bar{6}$06	14.9	-15.6	0.7
$\bar{8}$06	19.2	-18.6	-0.6
$\bar{10}$06	4.4	-3.6	0.8
$\bar{12}$06	<1.7	0.8	—
$\bar{14}$06	3.6	2.9	0.7
$\bar{16}$06	4.9	-4.0	-0.9
$\bar{18}$06	<1.2	0.9	—
$\bar{20}$06	1.7	0.5	1.2
$\bar{2}$07	10.7	-10.6	-0.1
$\bar{4}$07	14.3	-14.6	0.3
$\bar{6}$07	4.2	4.1	0.1
$\bar{8}$07	2.0	1.9	0.1
$\bar{10}$07	2.8	2.2	0.6
$\bar{12}$07	4.9	-4.0	-0.9
$\bar{14}$07	<1.4	0.7	—
$\bar{16}$07	1.9	0.6	1.3
$\bar{18}$07	7.6	-7.7	0.1
$\bar{2}$08	3.2	3.4	-0.2
$\bar{4}$08	2.7	2.1	0.6
$\bar{6}$08	<1.5	0.1	—
$\bar{8}$08	3.9	-2.8	-1.1
$\bar{10}$08	<1.4	0.5	—
$\bar{12}$08	<1.2	0.3	—
$\bar{14}$08	8.4	-8.4	0.0
$\bar{2}$09	<1.1	-0.8	—
$\bar{4}$09	2.0	-1.6	-0.4
$\bar{6}$09	<1.1	0.7	—
$\bar{8}$09	<1.0	-0.1	—
$\bar{10}$09	6.6	-6.7	0.1
110	17.2	16.8	0.4
210	51.1	-54.1	3.0
310	53.2	54.5	-1.3
410	4.2	-3.3	-0.9
510	1.7	-1.3	-0.4
610	14.4	-14.8	0.4
710	7.8	-7.1	-0.7
810	7.1	8.1	-1.0
910	4.6	-4.4	-0.2
1010	4.1	4.1	0.0
1110	10.7	9.7	1.0
1210	4.4	-3.9	-0.5
1310	2.5	-2.0	-0.5
1410	2.2	1.5	0.7
1510	3.7	-3.3	-0.4
1610	1.9	-1.6	-0.3
1710	6.8	6.3	0.5
1810	2.4	-2.4	0.0
1910	3.5	3.0	0.5
2010	1.6	-1.6	0.0
2110	<1.4	0.2	—
2210	2.5	-2.0	-0.5
2310	<1.0	-0.6	—
020	10.5	-2.3	-2.2
120	9.6	-10.0	0.4
220	<1.1	1.5	0.4
320	20.8	-18.5	-2.3
420	10.8	10.6	0.2
520	8.3	6.7	1.6
620	1.4	2.1	-0.7
720	10.0	9.3	0.7
820	3.0	3.3	-0.3
920	7.0	-7.9	0.9
1020	5.1	-5.3	0.2
1120	6.9	-6.2	-0.7
1220	4.1	-4.2	0.1
1320	2.1	-2.0	-0.1
1420	3.6	2.9	0.7
1520	4.8	4.3	0.5
1620	2.1	-2.5	0.4
1720	<1.7	-1.2	—
1820	2.4	1.8	0.6
1920	4.0	-3.3	-0.7
2020	1.6	1.6	0.0
2120	1.4	-0.9	-0.5
2220	<1.0	0.9	—

Index	Fo	Fc	ΔF
130	3.6	3.3	0.3
230	16.4	15.8	0.6
330	4.5	-2.7	-1.8
430	<1.4	0.8	—
530	4.4	-5.5	1.1
630	8.1	-8.3	0.2
730	2.7	2.3	0.4
830	2.1	-1.8	-0.3
930	12.1	-11.8	-0.3
1030	3.0	-3.5	0.5
1130	8.9	-8.9	0.0
1230	<1.7	0.7	—
1330	3.6	3.3	0.3
1430	4.0	-4.0	0.0
1530	3.7	3.2	0.5
1630	<1.6	-0.5	—
1730	2.1	-1.3	-0.8
1830	2.2	2.7	-0.5
1930	1.5	-1.3	-0.2
2030	1.4	-1.2	-0.2
040	4.3	-4.2	-0.1
140	<1.7	1.3	—
240	<1.7	-0.4	—
340	3.6	-3.0	-0.6
440	7.4	6.2	1.2
540	<1.7	-1.4	—
640	9.4	-9.6	0.2
740	4.9	-5.1	-0.2
840	18.8	-18.5	-0.3
940	3.3	-4.6	1.3
1040	<1.7	0.6	—
1140	5.8	6.0	-0.2
1240	<1.7	0.3	—
1340	2.9	2.2	0.7
1440	3.4	-2.7	-0.7
1540	<1.4	-1.1	—
1640	<1.3	1.2	—
1740	2.3	-1.8	-0.5
1840	1.3	1.3	0.0
150	4.8	4.5	0.3
250	2.5	-1.9	-0.6
350	8.5	-7.9	-0.6
450	<1.7	-1.7	—
550	8.1	-7.1	-1.0
650	9.3	-8.5	-0.8
750	3.0	1.7	1.3
850	2.4	3.1	-0.7
950	<1.5	0.1	—
1050	5.7	4.4	1.3
1150	6.0	-4.8	-1.2
1250	1.6	1.1	0.5
1350	3.4	-3.1	-0.3
1450	2.9	2.4	0.5
060	2.5	-2.0	0.5
160	<1.3	-0.1	—
260	<1.2	0.3	—
360	2.2	-1.6	-0.6
460	2.1	-1.5	-0.6
560	1.1	0.3	—
660	1.8	-1.0	-0.8
760	<0.9	-0.1	—

in $R = 44.9\%$ for the observed reflections. Refinement proceeded through one additional F_o synthesis and ten ΔF syntheses.

From the structure projected on (010) and approximate expected bond lengths, y coordinates were assigned. Calculation of the 48 most intense F_{hk0} reflections gave $R = 35.4\%$. Only these most intense reflections were used for the first F_o and first four ΔF syntheses. After these five refinement cycles, R stood at 7.2% for the above 48 reflections. Calculation of all observed F_{hk0} gave $R = 15.1\%$. From this point on, refinement proceeded through six ΔF syntheses, using complete $hk0$ data.

Values of the reliability index, R, based on all observed structure factors are given in Table 1. In Table 2 are listed individual atom temperature-factor para-

Fig. 2. (a, b) ΔF syntheses from which final coordinate changes were taken, and numbering of the atoms. Contours at intervals of 0.2 e.Å^{-2}, zero contour omitted, negative contours broken. (c, d) ΔF syntheses showing hydrogen atoms. Contours at intervals of 0.2 e.Å^{-2}, zero and negative contours broken. (e, f) ΔF syntheses showing electronic anisotropy. Contour interval 0.2 e.Å^{-2}, zero contour omitted, negative contour broken.

meters used in calculating final structure factors; F_o, F_c and ΔF appear in Table 3. From the coordinates of Table 4, the bond lengths and angles of Table 5 were calculated. Final F_o syntheses are shown in Figs. 1(a) and 1(b) and difference maps from which final corrections were taken in Figs. 2(a) and 2(b).

Table 4. *Atomic coordinates*

	x/a	y/b	z/c
C_1	0·0087	0·1140	0·9393
C_2	0·0548	0·0260	0·7944
C_3	0·0694	0·2596	0·6745
C_4	0·1422	0·3602	0·4279
C_5	0·1887	0·2460	0·2945
C_6	0·2096	0·4508	0·1612
N	0·1122	0·1826	0·5324
O	0·1325	0·6072	0·4520
H_1	0·040	0·807	0·133
H_2	0·040	0·252	0·040
H_3	0·025	0·888	0·710
H_4	0·107	0·950	0·857
H_5	0·017	0·333	0·607
H_6	0·102	0·415	0·757
H_7	0·119	0·978	0·510
H_8	0·152	0·101	0·210
H_9	0·233	0·121	0·363
H_{10}	0·167	0·545	0·080
H_{11}	0·245	0·595	0·237
H_{12}	0·238	0·333	0·060

Table 5. *Bond lengths and angles*

C_1–C_1'	1·512 Å	C_1'–C_1–C_2	113·3°
C_1–C_2	1·529	C_1–C_2–C_3	111·2
C_2–C_3	1·512	C_2–C_3–N	112·8
C_3–N	1·458	C_3–N–C_4	123·9
N–C_4	1·346	N–C_4–C_5	116·9
C_4–C_5	1·512	C_4–C_5–C_6	113·7
C_5–C_6	1·509	N–C_4–O	118·5
C_4–O	1·255	C_5–C_4–O	124·5
N–H $\cdots$ O	2·951		

Discussion

All H atoms except H_7 are tetrahedrally bonded to C atoms. Coordinates for these H atoms were determined by using a C–H bond length of 1·1 Å and tetrahedral angles. The methyl group was rotated about the C_5–C_6 bond until a reasonable match between methyl H atoms and the corresponding peaks of the difference map on (010) resulted. H_7 was placed on a line joining the N atom of one molecule with the O atom of the adjacent molecule, assuming a N–H bond length of 1·0 Å. Agreement between the positions of the H atoms thus chosen and the hydrogen peaks of the difference maps is indicated in Figs. 2(c) and 2(d). Agreement is rather poor in general and particularly so for H atoms of the propionyl group in projection along [001]. Nevertheless the essential correctness of the H atom positions is indicated. Because of the large thermal motion, much better H atom positions would result by using diffraction data collected at liquid nitrogen temperature. Figs. 2(e) and 2(f) are difference maps showing the difference of electron density from that corresponding to McWeeny scattering factors (McWeeny, 1951) with a temperature factor $\exp[-4·0 \sin^2 \theta/\lambda^2]$. It is clear from Fig. 2(e) that in projection on (010) the direction of maximum vibration is essentially the same for all atoms and at right angles to the chain. Now in the projection along [001], Fig. 2(f), although all atoms are resolved, overlap is appreciable and the best direction (or directions) of

maximum vibration is not clear except for the O atom. For this reason and to simplify calculation, the direction of maximum vibration in projection along [001] was assumed to be parallel to a^*.

Fig. 3 indicates how overlap in a zigzag chain
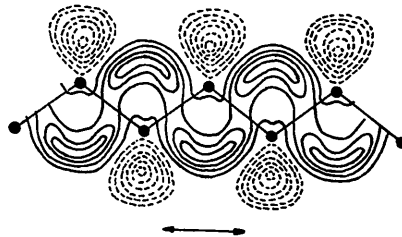
Fig. 3. ΔF synthesis for chain structure with direction of maximum vibration along chain ($\longleftrightarrow$); spherical atoms assumed in calculating F_c.

coupled with isotropic (or incorrect anisotropic) temperature-factor parameters may affect atomic coordinates. For this case, similar to the projection of HMBPA along [001], each line of atoms would be shifted toward the other and bond lengths systematically short would result. It can be seen that, depending on direction of maximum vibration, bond lengths could result that are systematically long or that alternate. It should be pointed out that three-dimensional results that do not take into account anisotropic thermal motion may not be entirely free of the effect.

The C–C bonds of the saturated chains of HMBPA are essentially constant and the average value is 'significantly' below the 1·544 Å C–C single bond in diamond. However, in calculating standard deviations of atomic coordinates on which the significance criteria are based (Cruickshank, 1949), one assumes random errors. Systematic errors in the data or in the treatment of the data may result in apparent differences where no real difference exists. The simplification used in calculating F_{hk0} probably accounts at least in part for the short C–C bonds. Since the primary purpose of this work was not to determine accurate bond lengths, it did not seem worthwhile to explore the matter further at this time.

The bond lengths C_3–N, N–C_4 and C_4–O are close to expected values, and all bond lengths agree well with those of corresponding bonds in N,N'-hexamethylenebisacetamide (Bailey, 1955).

As would be expected from the bond lengths, the bond angles of the tetrahedral C atoms in the chain are a little greater than expected and appreciably greater than 109° 28'. All bond angles are close to the corresponding angles of N,N'-hexamethylenebisacetamide, except for N–C_4–O and C_5–C_4–O. This difference is to be attributed to differences in packing and hydrogen bond energies. Deviations from ideality of bond angles about the trigonal C_4 and N atoms result in a considerable bend in the molecule at the amide linkage.

Molecules are bound together in molecular ribbons along b by N–H $\cdots$ O hydrogen bonds shown schematically in Fig. 4. It is this molecular arrangement that
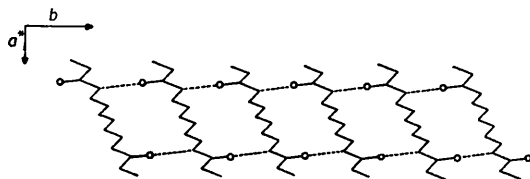

Fig. 4. Schematic representation of molecular ribbon.

results in cutting anisotropy of the crystals, i.e. easy cutting parallel to b but only with difficulty normal to b.

We wish to express our thanks to Mr Charles Chaney, who assisted in the calculations. We wish to acknowledge financial support from the National Institute of Health contract A-858, the Fund for Biological and Medical Research of the University of Washington and the U.S. Army Quartermaster Corps Contract No. Da 19-129-QM-523.

References

BAILEY, M. (1955). *Acta Cryst.* **8**, 575.
CRUICKSHANK, D. W. J. (1949). *Acta Cryst.* **2**, 65.
JENSEN, L. H. (1956). *J. Amer. Chem. Soc.* **78**, 3993.
McGUIRE, T. R. (1949). Ph.D. Thesis, Yale University.
McWEENY, R. (1951). *Acta Cryst.* **4**, 513.
MADDIN, R. & ASHER, W. R. (1950). *Rev. Sci. Instrum.* **21**, 881.
WIEBENGA, E. H. & SMITS, D. W. (1950). *Acta Cryst.* **3**, 265.

Short Communications

Contributions intended for publication under this heading should be expressly so marked; they should not exceed about 500 words; they should be forwarded in the usual way to the appropriate Co-editor; they will be published as speedily as possible; and proofs will not generally be submitted to authors. Publication will be quicker if the contributions are without illustrations.

A method of eliminating the primary extinction effect in electron diffraction. By GORO HONJO and NORIHISA KITAMURA, *Tokyo Institute of Technology, Oh-okayama, Meguroku, Tokyo, Japan*

It has been reported by a number of workers that the intensity of electron diffraction by a crystal sometimes deviates from the value calculated by the kinematical theory of diffraction (Yearian & Howe, 1935; Ornstein, Brinkman, Hauer & Tol, 1938; Tol & Ornstein, 1940; Lennander, 1954). Blackman (1939) ascribed it to the dynamical diffraction effect, or the primary extinction effect. On the basis of the experiment of Jamzin (1949), Pinsker (1949) published an opinion contradicting Blackman. Kuwabara (1957), however, recently performed an experiment similar to that of Jamzin on evaporated films of some metals and salts, and recognized that an appreciable extinction effect occurs even for quite small crystallites. Therefore it is very important in electron-diffraction structure analysis to have a method of eliminating the primary extinction effect. One promising method has been recently proposed by Nagakura (1957), utilizing Wilson's intensity statistics combined with the current theory of the primary extinction effect (Blackman, 1939).

Bacon & Pease (1953) gave a method of eliminating the secondary extinction effect in neutron diffraction by the extrapolation of intensities measured at various wavelengths to the wavelength zero. A similar method may be applied also to electron diffraction.

According to the result of the dynamical theory applied to a parallel-plate crystal (Blackman, 1939), the intensity of a reflexion is given by

$$I \propto f(A) \cdot |F|^2, \tag{1}$$

where F is the structure factor and $f(A)$ is the primary extinction coefficient defined by

$$f(A) = \frac{1}{A} \int_0^A J_0(2x)dx .$$

Here J_0 is the zero-order Bessel function, $A = c|F|H\lambda$, c is a constant, H is the thickness of the crystal and λ is the wavelength. The function $f(A)$ can be approximated by $\exp(-\frac{1}{3}A^2)$ for $A \leq 2$ within an error less than 1%. Then (1) can be rewritten as

$$\ln I = \ln |F|^2 - \frac{1}{3}c^2|F|^2H^2\lambda^2 + \text{const.} \tag{2}$$

Thus, $\ln I$ should be linear to λ^2 with a gradient $\frac{1}{3}c^2|F|^2H^2$, and the value of $\ln I$ extrapolated to $\lambda = 0$ should give the kinematical value of I.

The above theory may not hold exactly for crystallites of complicated shapes in practical specimens. We can, however, anticipate that the use of the $\ln I - \lambda^2$ plot will give a practical method of obtaining the kinematical intensity.

An experimental observation was carried out for poly-